Application of Computational Fluid Dynamics in Examining the Filtration Efficacy of Fine and Coarse Particles in a Baffle integrated-Vertical Ventilation Duct

Chau Hoang Bao
University of Natural Resources and Environment

Le Tan Dat
University of Natural Resources and Environment

Nguyen Dang Khoa
Interdisciplinary Graduate School of Engineering Sciences, Kyushu University

Hua Minh Quang
University of Natural Resources and Environment

他

https://doi.org/10.5109/5909101

出版情報：Proceedings of International Exchange and Innovation Conference on Engineering & Sciences (IEICES). 8, pp.259-264, 2022-10-20. Interdisciplinary Graduate School of Engineering Sciences, Kyushu University
バージョン：

Proceedings of the 8th International Exchange and Innovation Conference on Engineering & Sciences (IEICES 2022)

Application of Computational Fluid Dynamics in Examining the Filtration Efficacy of Fine and Coarse Particles in a Baffle integrated-Vertical Ventilation Duct

Chau Hoang Bao[1], Le Tan Dat[1], Nguyen Dang Khoa[2], Hua Minh Quang[3], Tran Huynh Chieu[4], Nguyen Lu Phuong[1*]
[1,3,4] University of Natural Resources and Environment, Ho Chi Minh City, Vietnam
[2] Interdisciplinary Graduate School of Engineering Sciences, Kyushu University, Japan
*Corresponding author email: nlphuong@hcmunre.edu.vn

Abstract: *According to past research, vertical ventilation ducts could improve particle deposition rate. The removal efficiency could be achieved up to 80% for coarse particles and approximately 10% higher for fine particles. To enhance particle removal efficiency, we designed ventilation ducts with baffles to compare their particle removal performance to that of prior ventilation ducts without baffle. Three different designs were generated, one model with two baffles and two models with four baffles, which were also compared the effects on the particle transport mechanisms. When comparing the effectiveness of particle removal by using the simulated results, we found that vertical ventilation ducts with baffles increased particle deposition and reduced particle escape compared to duct without baffle. The percentage of particles retained in the ventilation duct increased proportionally with particle size in all cases. In comparison to different designs, integrating four baffles in opposite directions proposed a better filtering efficiency of particles.*

Keywords: Computational fluid dynamics (CFD); Vertical ventilation duct; Fine particle; Filtration efficiency.

1. INTRODUCTION

In recent years, ambient air pollution from particulate matter (PM) has become a severe problem in urban areas. These suspended toxic particles could enter the indoor environment due to natural ventilation and degrade indoor air quality [1]. People spent around 80-90% of their time in a closed climate [2][3][4], and they could be exposed to particles originating from the external environment that penetrated into the indoor environment. Long-term exposure to particulate matter (PM) might exert respiratory-related diseases such as asthma, laryngeal cancer, and lung cancer [5]. According to the report of WHO, in 2020, an estimated 24% of deaths worldwide were related to environmental quality, and a total of approximately 8 million deaths were caused by indoor and outdoor air pollution; of which, 3.8 million deaths were related to indoor air quality, and 4.2 million deaths were due to exposure to fine particulate matter. Therefore, ventilation was considered an important factor in reducing indoor particulate concentrations originating from ambient air.

Many prior studies indicated that inefficient natural ventilation design negatively influences interior air quality. Most concentrated on the I/O ratio, which was simple to comprehend the interaction between indoor and outdoor air quality [6]. However, the vertical ventilation duct could reduce the concentration of aerosol particles by settling into the duct lines [7]. Hence, this decreased the operational power of the particle filter in the rear air conditioning systems, increasing equipment maintenance time as well as cost efficiency and equipment utilization time. Human exposure to harmful outdoor aerosol particles could be reduced [8]. Besides, the square tube design allowed particles to adhere to the surface of the duct under the gravitational force and other external forces. The design of the vertical ventilation duct partition wall was also taken into account to improve the possibility of particles impacting the pipe wall, adding to the removal of coarse particles when passing through the ventilation duct [9].

Currently, Computational Fluid Dynamics (CFD) has been widely adopted as an alternative means for predicting the behavior of fluid flow and substances in complex geometries [10][11]. Besides, it has also been applied with some new research in the health field in the era of SARS-CoV-2 [12] or complex systems inside the human body [13] for reliable results. Therefore, vertical ventilation ducts were developed in this study utilizing the Computational Fluid Dynamics (CFD) approach to increase ability to remove particulate pollution from the outside of the house. Simultaneously, the study applied Eulerian and Lagrangian approaches to predict the airflow pattern and movement of particles in three different ventilation duct types. The velocity distribution, pressure, propagation, and particle removal efficiency of various ventilation duct designs were compared and assessed.

2. METHODOLOGY

2.1 Generation of vertical ventilation duct integrated with baffles

The vertical ventilation duct was designed based on the actual size from the ventilation duct models for level four houses in Japan. The vertical duct model was built into six modules with a total height of 2,200 mm: 1. the input cylinder part, 2. the output cylinder part and the straight square tube consisting of four compartments (dimension: L x H x W = 100 x 100 x 500 mm); in particular, baffles were designed by attaching to each midpoint of the compartment (baffles dimension: L x W x H = 100 x 50 x 5 mm). (Figure. 1a)

In this paper, three different designs were generated. In the case of model A, two baffles were designed in the opposite direction at compartment 1 and compartment 4 in the model. Case B with four baffles integrated into the same direction and Case C was similar to Case B in terms of number and distance between the baffles but different in the order of placing the baffles (zigzagged).

2.2 Grid design for three vertical duct

The domain of interest was discretized using the finite volume method (FVM). Specifically, the type of the structural elements (hexagonal elements) was applied, which has been adopted to deliver high accuracy in simulation and reduce the computational cost, as shown in Figure 2. In addition, the first layer height of 10^{-3} m

was confirmed y^+ less than 1 and was built adjacent to the boundary wall to enhance the accuracy of airflow and discrete phase in this region.

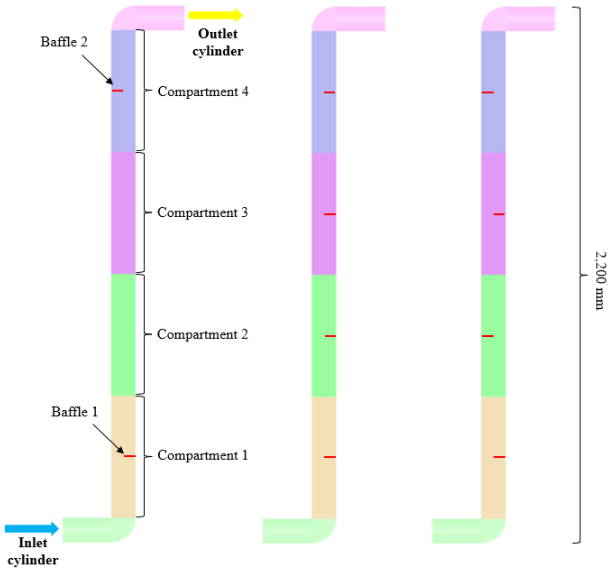

(a) Model A (b) Model B (c) Model C

Fig. 1. Outline of the vertical ventilation duct with two baffles (a) model A, four baffles in the same direction (b) model B, and four baffles in a different direction (c) model C.

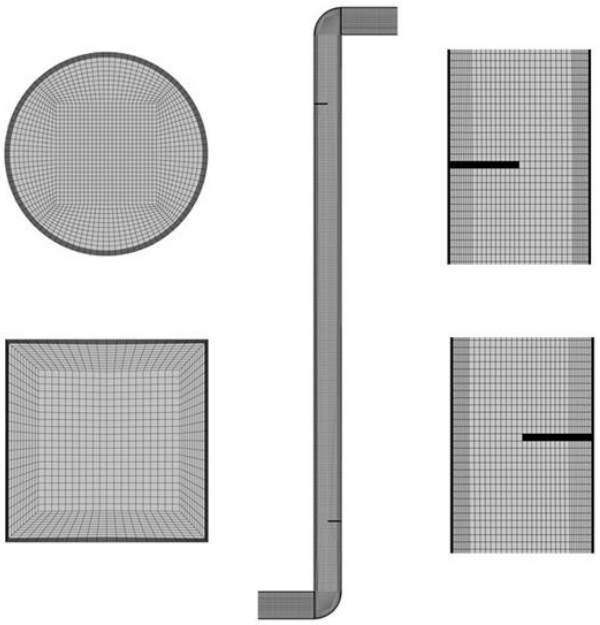

Fig. 2. The longitudinal section at the center position and cross-section at parts of baffled vertical ventilation ducts (model A).

2.2 CFD technique

2.2.1 Airflow simulation

The airflow patterns were simulated using the Eulerian method, in which a set of Reynolds Averaged Navier-Stokes-RANS equations (Equations 1 and 2) was solved for each control volume in the domain of interest. The low Reynolds types k-ε turbulent model was applied to account for the closing problem of the RANS equation.

$$\frac{\partial \overline{U}i}{\partial x_i} = 0 \tag{1}$$

$$\frac{\partial \overline{U_i}}{\partial t} + \frac{\partial}{\partial x_j}\left(\overline{U_i}\,\overline{U_j}\right) = -\frac{1}{\rho_g}\frac{\partial \overline{p_g}}{\partial x_i} + \nu\frac{\partial^2 \overline{U}i}{\partial x_j^{\,2}} - \frac{\partial}{\partial x_j}\left(\overline{u_i' u_j'}\right) \tag{2}$$

Table 1. Numerical boundary conditions

Parameters	Information
Algorithm	SIMPLE
Convection term	Second-order upwind
Inflow boundary	V_{in} = 0.3 m/s and Turbulent intensity = 10%
Wall condition	Trap (perfect sink)
Turbulent model	Low Renoyld k - ε model (Abe-Kondo-Nagano model)

2.2.1 Particle transportation simulation

This study applies the Lagrangian method to simulate the trajectories of particles. The simulation was based on Equation 3.

$$\frac{d\vec{u}_p}{dt} = \frac{18\mu}{\rho_p d_p^2}\cdot\frac{C_D\cdot Re_p}{24}\left(\vec{u}-\vec{u}_p\right) + \frac{\left(\rho_p-\rho\right)}{\rho_p}\cdot\vec{g} + \vec{F}_S \tag{3}$$

The left hand side of Equation 3 represents the force of inertia with the particle's velocity. On the right hand side of the formula, the first term is the drag force with the Drag coefficient, and the Correlated Reynolds coefficient is determined by Equations 4 and 5.

$$C_D = \frac{24(1-1.6807)Re_p^{0.6529}}{Re_p} - \frac{0.8271\cdot Re}{8.8798+Re_p} \tag{4}$$

$$Re_p = \frac{\rho\left|\vec{u}p-\vec{u}\right|d_p}{\mu} \tag{5}$$

The right-hand side of Equation 3 represents gravity, the density of air and particle. The third part is the Saffman lift force per unit mass, respectively.

$$\vec{F}_S = 5.188\frac{\nu^{1/2}\rho d_{ij}\left(\vec{u}-\vec{u}_p\right)}{\rho_p d_p\left(d_{lk}d_{kl}\right)^{1/4}} \tag{6}$$

The 10,000 monodispersed particles with an aerodynamic diameter ranging from 1-100 μm were released at the inlet of the model. The density of the particles was assumed at 1000 kg/m^3. The trap boundary condition was set for the wall and baffle, which means the particles have no possibility to rebound into the flow after interacting with the wall and baffles.

In addition, the residence time of the particles inside the vertical duct was calculated according to the following formula:

$$t = \frac{V}{Q_{in}} \quad (7$$

Terminology: t: The nominal time constant, V: Total model volume, Q_{in}: Inlet flow
With the above Equation, the particle time constant at the inlet velocity of 0.3 m/s for the three models is 10.45s, 10.41s, and 10.41s, respectively.

3. RESULTS AND DISCUSSIONS

3.1 Airflow distribution in the model

The characteristic of airflow patterns in the mid-plane position of the three models is shown in Figure. 3. The color scale denotes the normalized magnitude of velocity (u/u_{in}), the red color indicates the highest velocity, and the blue represents the lowest value.
From the results, the inlet air quickly passed through the inlet cylinder before suddenly bending 90-degree following the structure of the vertical ventilation duct. This geometric feature created the Coanda effect describing the attachment of the fluid flow to the convex surface and forming the low velocity and curvature flow on the opposite side, as shown in Figure. 3. A sudden acceleration of the airflow is observed at the left inner-wall due to the appearance of the first baffle position (350 mm) in the three models. This can be attributed to the cross-section of the ventilation duct at this position being reduced by 50% compared to the original duct. Simultaneously, the velocity in the right inner-wall was significantly lower than its counter partner in the three models. After the acceleration, the airflow showed rapid deaccelerating and uniform distribution in model A (Figure. 3a). However, the increment of several baffles in models B and C demonstrated the continuous acceleration of fluid at the position of baffles (Figure. 3b and 3c). The difference in locating the baffle direction in models B and C either affected the airflow distribution or the maximum velocity magnitude. Specifically, a higher velocity was observed at the baffle position in model C compared to model B. At the highest altitude baffle (750 mm), because of the discrepancies in placing the baffle direction, the airstream in model B was adjacent to the convex wall and escaped from the ventilation duct (Figure. 3b).
In contrast, the result of airflow models A and C show the attachment of the airstream in the right inner wall (Figure. 3a and 3c). Though, the low velocity was found in the bottom of the outlet cylinder in the three models. These results imply that the number or the position of baffles integrated into the vertical ventilation duct can profoundly impact the distribution and acceleration/deacceleration characteristics of airstream moving in the duct; consequently, it may exert a particular impact on the particle transportation.

3.2 Particle residence time in the model

Figure 4 shows the fraction of particles escaping from the vertical ventilation duct outlet following the time function. The real resident time of particles in the vertical ventilation duct was extracted at the outlet of the models.

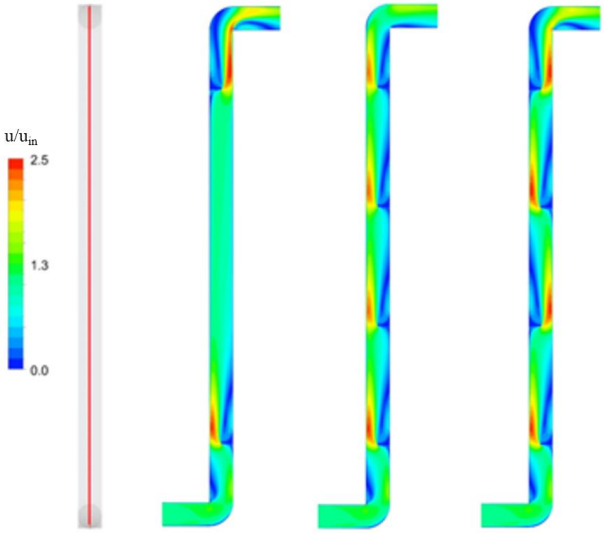

(**a**) model A **(b)** model B **(c)** model C

Fig. 3. Comparison of normalized airflow distribution in three models at an inlet velocity of 0.3 m/s.

In general, most of the large particles (100 μm) were trapped in the inlet pipe by gravity, resulting in the highest retention time for these particles; therefore, the residence time was long. The residence time of these particles is not shown in these graphs.
Following the results, at the calculated resident time, most of the investigated particle size (1-50 μm) remained in the ventilation duct (around 7,500 particles). These phenomena were observed in the three models. However, from the calculated timeline, the number of particles exiting the model through the outlet increased rapidly, especially in model A (Figure. 4a), which showed a fraction of 76.5% in the case of 1 micron-sized particle (corresponding to 7,650 particles). This fraction was dramatically reduced to 3.2% (corresponding to 320 particles) in the case of 50 μm particles. Almost identical data was also recorded in the model B (Figure 4b), in which the number of particles that escaped through the outlet at the end of calculation time (the 30s) was 7,660 particles (76.6%) for 1 mm particles, and that of 50 mm particles was 4,000 particles (4%). Nonetheless, the percentage of particles escaping from the vertical ventilation duct in model C was lower than that of models A and B (Figure 4a and 4b) in the cases of 1-30 μm particles. NotabThe recorded percentage at the end of calculation time was 63.4, 51, and 23,9% for particle sizes of 1, 10, and 30 μm, respectively. This implies that the higher number of particles remained in model C at the given specific calculation time compared to models A and B.
These results indicate that the retention/escape of particles was significantly dependent on the particle size and the design of the vertical ventilation duct. Therefore, obtained results can support the decision-making process for the optimized design of the vertical ventilation duct.
Figure 4 The graph shows the rate of particles escaping over the time constant at V_{in} = 0.3 m/s in three models of vertical ventilation ducts with baffles.

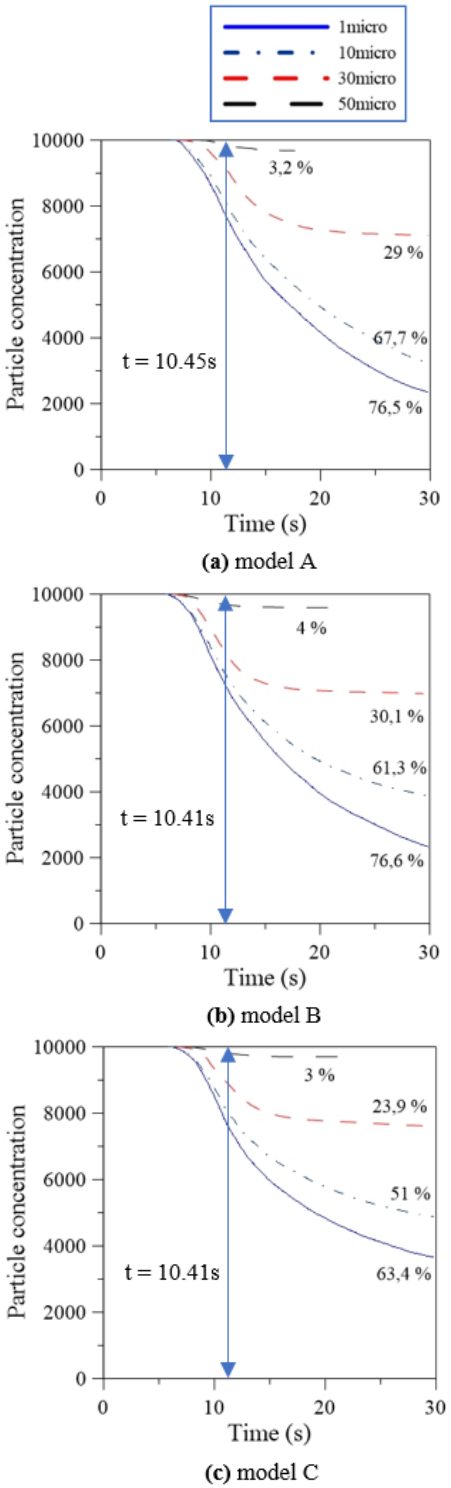

Fig. 4. The resident time of fine and coarse particles at the V_{in} = 0.3 m/s in three models of vertical ventilation ducts with baffles.

3.3 Visualization of retained particles in the vertical ventilation duct

The 3D visualization of retained particles is shown in Figure. 5. Only the 1 micrometer-sized particles are depicted herein at the inlet velocity of 0.3 m/s.

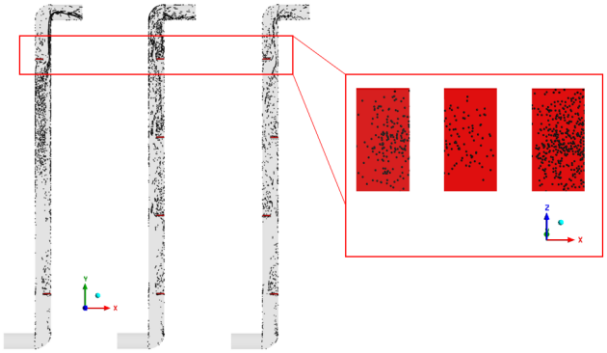

(a) **(b)** **(c)**

Fig. 5. Location distribution of particles with diameter 1 μm at V_{in} = 0.3 m/s in three models.

Generally, the results demonstrate a small number of particles that were retained at the inlet cylinder and the 90° bend region after entering the ventilation duct in the three models. These phenomena can be attributed to the fact that the 1 micron-sized particles with low inertia and gravitational characteristic could easily pass through the entrance region. As encountering the first baffle from the bottom, the circulation of particles is observed in the low-velocity region (on the right side of the ventilation duct) after passing through the baffle in the three models. For model A (Figure. 5a), the particles smoothly followed the airstream to the second baffle before exhausting at the outlet. In models B and C (Figure. 5b and 5c), the movement of particles was continuously struggled by other baffles, and the circulation phenomena after bypassing the baffles were still recorded. In addition, in these cases (models B and C), the continuous acceleration or the change of flow direction either facilitated the contact of particles with the lower surface of the baffle, making them trapped in these regions, especially for the particles with high inertia impaction which requires longer relaxation time to adjust their movement following the airstream. Therefore, in terms of mechanism, these results indicate that the integration of baffles can hamper the smooth movement of particles throughout the vertical ventilation duct which may improve the filtration efficiency.

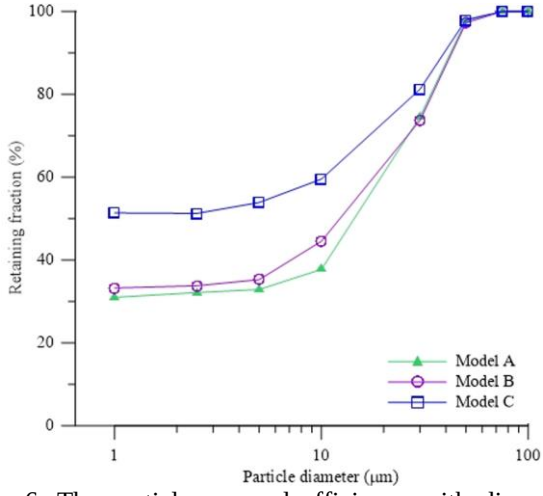

Fig. 6. The particle removal efficiency with diameter from 1 to 100 μm at V_{in} = 0.3 m/s in the three models.

3.4 Particle removal performance and compare results with previous research

As discussed above, the integration of baffles may mechanistically propose better filtration efficiency; however, it also raises a concern about the design of vertical ventilation duct-integrated baffles, including two factors, i.e., number of baffles and placement type. Therefore, the following discussion aims to evaluate the particle removal performance of three vertical ventilation duct designs, which supports the decision-making for an optimal design. In this study, the deposition of particles in the ventilation duct was impacted by gravitation and inertia impaction. A perfect trap boundary conditions at the baffles were defined that result in the deposition of particles interacting with the baffles, and the remaining particle will continue to proceed with the airflow.

The particle removal efficiency was plotted against the particle size for the three models at the inlet velocity of 0.3 m/s, as shown in Figure. 6a. In general, the particle removal efficiency increased proportionally with the particle size in the three models. Specifically, in terms of particles <10 μm, a slight increment of particle filtration efficiency is observed; in contrast, the removal efficiency rapidly increased in the case of coarse particles (d>10 μm). This is attributed that the gravitational effect governing the coarse particles; thus, the particles in this size range had less possibility to transport to the exhaust outlet of the vertical ventilation duct. Another factor is the integration of baffles, which hamper the smooth movement of particles throughout the ventilation duct. Particularly, the increment of baffle number to four (model B and C) proposed the better removal efficiency of particles <10 μm. Nonetheless, the placement of baffles also significantly affected the filtration efficiency. In which the same direction integration (model B) shows a higher removal efficiency (around 3-7 %) compared to model A, while that of model C demonstrates a much higher deposition compared to models A and B (around 8-20 %). The opposite placement of baffles in model C exerted certain obstacles to the transportation of particles in the ventilation duct. Apart from the fine particles, the removal efficiency was almost identical in the three models for particle size larger than 50 μm since the gravitational effects dominantly acted on the particles and prevented the particles from entering the baffle region; thus, the impact of baffle integration is not observed in this size range.

In addition, this study was conducted for particles under isothermal conditions. The results were compared with the previous research in a ventilation duct without baffle by Phuong and Ito, 2012 [9]; The results show that with the identical inlet velocity (V_{in} = 0.3 m/s) and particle size, the models with baffles in this study showed a higher particle retention rate compared to the previous study on the model without baffles. Specifically, for model C, the retaining fraction was higher of 5-15% than in models A and B. For coarse particles (>50 μm), the homogeneous retaining fraction was recorded in the three models, because at the low inlet velocity of 0.3 m/s, the particles had insufficient kinetic energy to escape the vertical ventilation duct, and also shows that the coarse particles are almost always trapped in the model with or without baffle.

These results indicate that the increment of baffle number had a certain effect on the removal efficiency, in which the more baffles integrated, the better filter ability. However, the placement of the baffles and the inlet velocity variation significantly contributed to filtering the particles from inlet air, especially the fine and coarse particles with a diameter smaller than 10 μm. Nonetheless, the outperformance of model C at particle retaining rate pointed out that this model's design is optimal.

4. CONCLUSION

3D models of vertical ventilation ducts with baffles were built and simulated using CFD technology to qualitatively and quantitatively predict the distribution of airflow and particle removal efficiency in the ventilation duct model. The airflow pattern showed fluid acceleration at the baffle region, resulting in the low velocity on the opposite side. The simulation results show that particles with a diameter of fewer than 10 μm tend to follow the airflow and exit the tube, while particles larger than 10 μm were mostly retained in the vertical ventilation duct. In terms of removal efficiency, with an inlet velocity of 0.3 m/s, for particles have a diameter < 10 μm, the particle removal rate in model C is approximately 1.5 times higher than that of model A (two baffles in the opposite direction) and model B (four baffles in the same order). Although baffles integrated designs performed particle filtration capacity dependent on the inlet velocity; however, this paper has confirmed the optimization in particle retention of model C with four baffles placed in the opposite direction.

5. REFERENCES

[1] B. Blocken, LES over RANS in building simulation for outdoor and indoor applications: A foregone conclusion?, Building Simulation 11 (2018) 821–870.

[2] M. Hajdukiewicz, M. Geron, M. M. Keane, Calibrated CFD simulation to evaluate thermal comfort in a highly-glazed naturally ventilated room, Build. Environ. 70 (2013) 73–89.

[3] P. H. Shaikh, N. B. M. Nor, P. Nallagownden, I. Elamvazuthi, T. Ibrahim, Robust stochastic control model for energy and comfort management of buildings, Aust. J. Basic Appl. Sci. 7 (2013) 137–144.

[4] A. A. Jamaludin, H. Hussein, A. R. M. Ariffin, N. Keumala, A study on different natural ventilation approaches at a residential college building with the internal courtyard arrangement, Energy Build. 72 (2014) 340–352.

[5] C. I. Davidson, R. F. Phalen, P. A. Solomon, Airborne Particulate Matter and Human Health: A Review, Aerosol Sci. Technol. 39 (2005) 737–749.

[6] C. Chen, B. Zhao, Review of relationship between indoor and outdoor particles: I/O ratio, infiltration factor and penetration factor, Atmospheric Environment 45 (2011) 275–288.

[7] W. J. Riley, T. E. McKone, A. C. K. Lai, W. W. Nazaroff, Indoor particulate matter of outdoor origin: importance of size-dependent removal mechanisms, Environ. Sci. Technol. 36 (2002) 200–207.

[8] T. L. Thatcher, A. C. K. Lai, R. Moreno-Jackson, R.

G. Sextro, W. W. Nazaroff, Effects of room furnishings and air speed on particle deposition rates indoors, Atmos. Environ. 36 (2002) 1811–1819.

[9] N. L. Phuong, K. Ito, Experimental and numerical study of airflow pattern and particle dispersion in a vertical ventilation duct, Build. Environ. 59 (2013) 466–481.

[10] H. Jiang, L. Lu, K. Sun, Experimental study and numerical investigation of particle penetration and deposition in 90 bent ventilation ducts, Build. Environ. 46 (2011) 2195–2202.

[11] B. Zhao, J. Wu, Modeling particle deposition from fully developed turbulent flow in ventilation duct, Atmos. Environ. 40 (2006) 457–466.

[12] H. Li, K. Kuga, N. D. Khoa, K. Ito, Effects of Initial Conditions and Parameters on the Prediction of SARS-CoV-2 Viral Load in the Upper Respiratory Tract Based on Host-Cell Dynamics, Int. Exch. Innov. Conf. Eng. Sci. 7 (2021) 155–160.

[13] S. Hanif, M. Sultan, T. Miyazaki, S. Koyama, Effect of drying air parameters on energy consumption in desiccant grain drying, Int. Exch. Innov. Conf. Eng. Sci. 3 (2017) 131–134.